High Efficiency Polymer Solar Cells with Long Operating Lifetimes

*Craig H. Peters, I. T. Sachs-Quintana, John P. Kastrop, Serge Beaupré, Mario Leclerc, and Michael D. McGehee**

The power conversion efficiency of organic photovoltaic (OPV) cells has increased from 4–5% in 2005[1,2] to 7.4%[3] and 8.3%[4] in 2010. The goal of a 10% single junction OPV device seems attainable[5] making the commercialization of OPV more realistic. With advances made on the efficiency front, the lifetime and reliability of OPV devices has come into focus.[6,7]

To date there has been considerable work done in understanding and quantifying the lifetime and degradation of bulk heterojunction solar cells (BHJs) based on poly(*para*-phenylene vinylene) (PPV)[8–11] and poly(3-hexylthiophene) (P3HT) polymers.[12–15] A comparison of OPV lifetime experimental results across different research groups has posed challenges due to the lack of standardized testing and reporting procedures; however, great strides were made in this regard during the most recent International Summit on OPV Stability (ISOS-3). Modules based on P3HT/fullerene BHJs have shown lifetimes of 5000 h when state-of-the-art encapsulation with a glass-on-glass architecture is used.[16] Assuming negligible degradation in the dark and 5.5 h of one-sun intensity per day, 365 days per year, this translates into an operating lifetime approaching three years. More recently P3HT/PCBM devices utilizing an inverted architecture have been shown to retain more than 50% of their initial efficiency after 4700 h of continuous exposure to one-sun intensity at elevated temperatures[17] and have exhibited a long shelf-life when stored in the dark in ambient conditions.[18,19] However, results to date have yet to show polymer based OPV lifetimes greater than 3–4 years.

Here we present a detailed operating lifetime study of encapsulated solar cells comprising poly[9'-hepta-decanyl-2,7-carbazole-alt-5,5-(4',7'-di-2-thienyl-2',1',3'-benzothiadiazole) (PCDTBT) in BHJ composites with the fullerene derivative [6,6]-phenyl C_{70}-butyric acid methyl ester ($PC_{70}BM$). PCDTBT/$PC_{70}BM$ solar cells achieved an efficiency greater than 6%,[20] making this one of a small number of polymers able to achieve this level of performance. We describe an experimental set-up that is capable of testing large numbers of solar cells simultaneously, holding each device at its maximum power point while controlling and monitoring the temperature and light intensity. Using this set-up we were able to compare the PCDTBT/$PC_{70}BM$ system with the well-studied P3HT/PCBM system and demonstrate a lifetime for PCDTBT devices that approaches 7 years, which is the longest reported operating lifetime for a polymer-based solar cell.

Figure 1 shows a typical efficiency decay pattern for polymer/fullerene BHJs employing a standard architecture with an organic hole-transporting layer as the anode (e.g., PEDOT:PSS) and a metal cathode (e.g., Ca/Al).[14,15] One typically observes a burn-in period characterized by an exponential loss in efficiency whose magnitude and duration can vary by polymer system, followed by a linear decay period that sometimes ends abruptly when the packaging fails. Device lifetime is typically measured in the linear decay period once burn-in has ended. Lifetime is defined as the point at which the efficiency from the beginning of the linear decay period has fallen to 80% of this initial value (T80 point).

Since testing and environmental conditions as well as sample preparation can vary greatly between laboratories, it is important for any lifetime study to use a sufficiently large sample size and to compare any new system against a well-studied system under identical aging conditions. In the current experiment, eight PCDTBT/$PC_{70}BM$ and eight P3HT/PCBM solar cells were prepared with average initial device efficiencies of 5.5 ± 0.15% and 4 ± 0.05%.All devices were protected by using encapsulation in a glass-on-glass architecture (see Experimental).

It is well known that UV radiation can induce defects and even chain scission in conjugated polymers.[21] To remove the harmful effects of UV, which will likely be filtered when OPV is commercialized, an LG sulfur plasma lamp, with little UV power but a strong spectral match to the AM 1.5 G solar spectrum in the visible wavelengths, was used. The lamp is highly

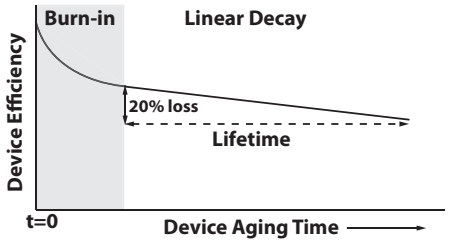

Figure 1. Typical decay curve of a polymer solar cell (solid black line) employing a standard architecture with an organic hole transporting layer as the anode and a metal (e.g., Ca/Al) as the cathode. The lifetime (dashed black) is defined by the point at which the efficiency has dropped by 20% from the start of the linear decay period. Both axes are linear.

C. H. Peters, I. T. Sachs-Quintana, J. P. Kastrop, Prof. M. D. McGehee
Department of Materials Science and Engineering
Stanford University
Stanford, CA 94305, USA
E-mail: mmcgehee@stanford.edu
Dr. S. Beaupré, Dr. M. Leclerc
Department of Chemistry
University of Laval
G1K 7P4 Quebec City, Quebec, Canada

DOI: 10.1002/aenm.201100138

efficient, has excellent stability and exhibits a long lifetime (~10 000 h).

It remains to be determined whether devices held at open-circuit voltage (V_{oc}) or short circuit current (J_{sc}) exhibit differing rates of degradation. However, solar cells in the field will be operating close to or at their maximum power point (Mpp). For this experiment each cell was held at its Mpp, which was dynamically adjusted every 5 s using a standard perturb and observe method implemented in the software.

The solar cells were fabricated, characterized, and stored in the dark for one week before being placed under the lamp. All devices experienced modest decay in J_{sc} while being stored in the dark (see Supporting Information). The solar cells were then aged at Mpp continuously for 4400 hours in air under one-sun intensity. Reflectors were constructed to provide uniform light intensity (±4%) over all devices. The intensity was calibrated using a National Renewable Energy Laboratory (NREL)-certified KG5 filtered silicon photodiode. The temperature was held at 37 °C using a water-heated copper plate. The temperature remained within ±2 °C throughout the duration of the experiment and varied by less than 0.5 °C from sample to sample. Both the light intensity and temperature were monitored every 5 s for each device. Current-voltage curves were taken every hour for the duration of the experiment.

Figure 2 shows the device characteristics over time for PCDTBT and P3HT devices. The curves are normalized to their initial values at the start of the aging process and the data points represent the average of every 100 h worth of data for the 8 devices for each polymer type (see Supporting Information for details on each device). The error bars for each point represent the maximum and minimum values for the devices at each of the data points. J_{sc} for both systems is linearly normalized for fluctuations in lamp intensity, which varied by less than ±5% over the course of the experiment.

The V_{oc} and FF of the PCDTBT devices remained remarkably stable for more than 4000 h after a burn-in period of ~400 h. The decay was then dominated by a slow decline in J_{sc} over the duration of the experiment. The abrupt drop in the PCDTBT upper errorbar for the FF at 2100 hours is due to one device experiencing a drop in FF over the course of several days. P3HT devices show similar behavior for J_{sc} and FF but experience a slow decline in V_{oc} throughout the experiment. Similarly made state-of-the-art encapsulated P3HT devices that were made into modules showed a drop in efficiency of 9.82% per 1000 h of continuous exposure, which is higher but comparable to what we have seen in this experiment.[16] The decline in both J_{sc} and V_{oc} of the P3HT devices result in a faster loss of efficiency when compared to PCDTBT devices. Though both systems show a burn-in period followed by a linear decay period (Figure 2d), it is clear that burn-in is more severe for PCDTBT devices.

The demarcation for the end of the burn-in period was chosen to be 1300 h for both sets of devices in Figure 2d. Linear regression was performed on the 3100 data points between 1300 and 4400 h and the linear fits were extrapolated out to the T80 point to find the lifetimes, as shown in Figure 1. A detailed analysis is included in the Supporting Information. The average lifetime for PCDTBT devices is found to be 6.2 years, assuming 5.5 h of one-sun intensity per day, which is twice that of the P3HT devices. There is no set guideline for choosing the point at which the burn-in period ends. Varying the end of the burn-in period between 1000 and 2000 h had almost no impact on the expected lifetime of the PCDTBT devices but made the lifetime of the P3HT devices range between 2.5 and 3.8 years. In either case the lifetime of the PCDTBT system was shown to be substantially longer than that of the P3HT system. It is important to note that the lifetime figures are for cells aged indoors. Under operating conditions in the field there are other influences such as natural thermal cycling and shading variations that need to be considered.

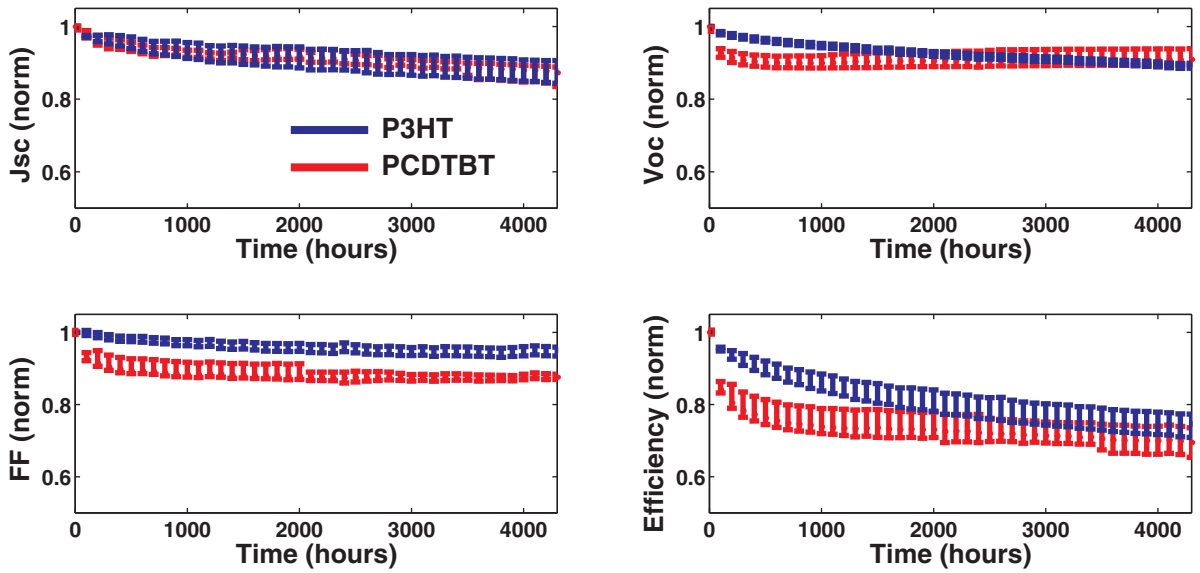

Figure 2. Device characteristics for PCDTBT (red) and P3HT (blue) solar cells over 4400 h of continuous testing. The curves are each normalized by the initial value at the start of the aging process. Each point represents the average of 100 h of data for 8 solar cells of each type.

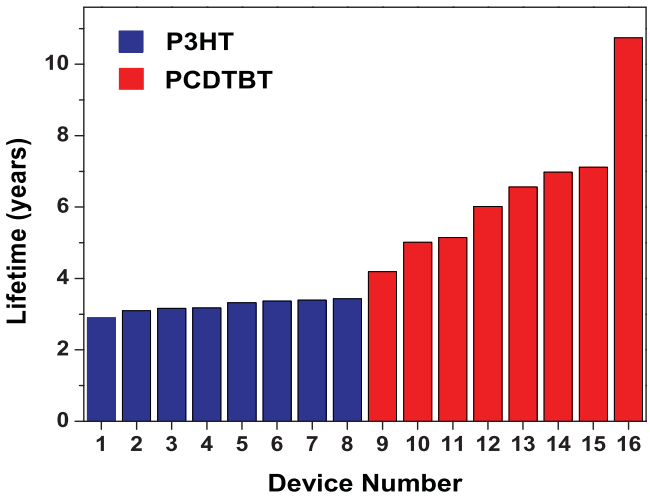

Figure 3. Ordered lifetimes of 16 devices. PCDTBT (red, 9–16) devices show substantially longer lifetimes but with a wider spread due to variation in J_{sc} over time while P3HT (blue, 1–8) solar cells show a narrower spread. Linear fits were used for each device using 3100 data points from 1300 to 4400 h and the lifetime was defined by the point where the initial efficiency at the 1300 h point drops by 20%.

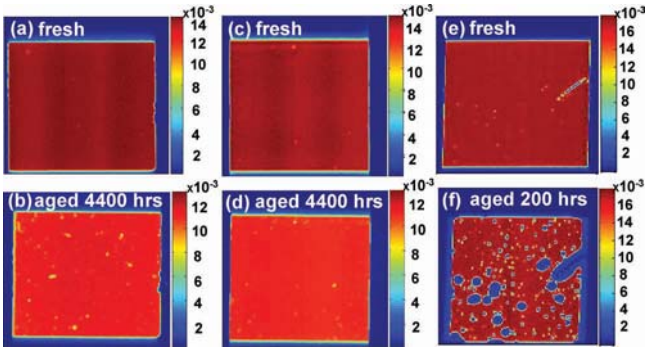

Figure 4. LBIC images of solar cells before and after aging under one-sun light intensity. Each image is a square area of 3.6 mm by 3.6 mm. (a) and (b) are images of a P3HT device before and after aging continuously for 4400 hours. The images show no loss of device area and the formation of smaller spots of low current. (c) and (d) are images of a PCDTBT solar cell before and after aging. No loss of device area is seen. (e) and (f) show the effects of encapsulation failure on a PCDTBT solar cell made identically to that in (c).

Figure 3 shows the lifetime of each device used in this study. The P3HT devices have a very narrow spread in lifetimes showing the reproducibility of P3HT system. Every PCDTBT device had a longer lifetime than the P3HT devices, though the PCDTBT devices had a larger spread in expected lifetimes due to variations in J_{sc} over time (included in the Supporting Information). One PCDTBT device displayed remarkably stable characteristics over the entire experiment leading to an expected lifetime approaching 11 years. It is important to point out that a reasonable amount of effort by the scientific community has been directed toward understanding and improving the stability and lifetime of the P3HT system[6] while very little effort has been directed toward optimizing the stability of the PCDTBT system. We expect optimization to narrow the spread in lifetimes seen in this experiment and increase the average value.

Laser beam induced current maps (LBIC) provide valuable insight into spatial distribution of J_{sc} and its subsequent degradation behavior by determining whether the loss is occurring uniformly over the sample or locally as in the case of pinhole formation.[22–26] **Figure 4** shows LBIC images for P3HT and PCDTBT devices before and after aging. Figures 4a-b show a uniform loss of current for a P3HT device. No loss of device area is seen, though the start of pinhole formation can be identified. Figures 4c–d show a fresh and aged PCDTBT device. Similar to the P3HT device there is a uniform loss of current with no loss of device area. However, fewer pinholes are seen. Finally, Figures 4e–f show the rapid formation of pinholes and a loss of device area for a PCDTBT device within 200 h of aging as the result of encapsulation failure. This device was not used in this study but is included here to show the importance of encapsulation on device lifetime.

In conclusion, PCDTBT/$PC_{70}BM$ solar cells have been shown to have a lifetime approaching seven years, which is the longest reported lifetime for a polymer-based solar cell and approximately twice that of the well-studied P3HT/PCBM system. The V_{oc} and FF of the PCDTBT system experience a rapid initial decay but then show remarkable stability for over 4000 h of continuous testing. Given the recent development of this polymer, little optimization of the architecture has been performed to promote the stability and enhance the lifetime of PCDTBT based solar cells. Through a deeper understanding of the decay mechanisms and further optimization of the architecture, both of which are underway, it seems reasonable to be able to reduce the burn-in loss and extend the lifetime, which would make OPV commercially viable.

Experimental Section

Solar cell fabrication: PCDTBT devices (St-Jean Photochemicals) were fabricated on glass substrates with the following structure: indium tin oxide (ITO)/poly(3,4-ethylenedioxythiophene)(PEDOT:PSS)/PCDTBT:$PC_{70}BM$/Ca/Al. The ITO (8 Ohm/sq from Thin Film Devices) coated glass substrate was ultrasonically cleaned in detergent, acetone and isopropyl alcohol, and subsequently dried overnight in an oven. The substrates were placed in a UV ozone chamber for 20 min prior to the deposition of PEDOT:PSS (AI 4083, HC Starck)via spin-casting from aqueous solution to form a 25 nm thick film. The substrate was annealed for 10 min at 140 °C in air and then transferred into a glove box to deposit the active layer and counter electrode. A solution containing a mixture of PCDTBT:$PC_{70}BM$ (1:4) (from M. Leclerc and Nano-C, respectively) in dichlorobenzene solvent with a concentration of 7 mg/mL was heated to 60 °C and subsequently spin-cast on top of the PEDOT/PSS layer to achieve an active layer of ~80 nm. The film was slow dried overnight in a covered Petri dish in the glove-box. Finally a Ca/Al (7 nm/100 nm) was deposited by thermal evaporation in a vacuum of about 1×10^{-6} mbar.

P3HT (Plextronics) and PCBM (Nano-C) in a 1.5:1 solution were used in dichlorobenzene. Substrates were prepared similarly to the PCDTBT devices. However, PV1000 HTL was used in place of PEDOT:PSS as the hole transport layer since this provides better device stability for the P3HT system. PV1000 HTL is spun in air to a thickness of 60 nm and is then baked on a hotplate for 15 min at 170 °C in a glove-box. The P3HT:PCBM active layer is then spin-cast in the glove-box to a thickness of 200 nm and baked on a hotplate in the glovebox at 175 °C for 30 min. Finally, a Ca (20 nm)/Al (200 nm) cathode is deposited in a thermal evaporation chamber at a base pressure of 1×10^{-6} mbar.

Solar cell encapsulation: A Resonetics 120 laser system operating at 248 nm wavelength was used together with an ATLEX-300-SI excimer laser (300 Hz repetition rate, 6 W average power, 20mJ maximum pulse energy) to remove organic layers from the contact and seal areas of the device. A cavity glass with an edge seal of UV curable epoxy acted as the top encapsulation layer. The epoxy used was Delo LP 651. It was deposited using a programmable Loctite 300 series bench top robot which defined a perimeter bead of glue in a square pattern in the center of the device. One Dynic getter was stuck to the cavity glass and the cavity glass was then pressed onto the part using the robot at the exact location where the perimeter of glue was applied. This resulted in an edge seal around the perimeter of the cavity glass. The part was then placed into a UVA LOC 1000 curer and the glue was cured at 50 mW/cm^2 power for 60 s. The devices remained in a nitrogen filled environment for 16 h to ensure that the glue cured fully before exposure to ambient conditions.

I-V characterization: Current density–voltage (*J-V*) measurements were carried out with a Keithley 2400 source meter and a 91160 300 W Oriel solar simulator equipped with a 6258 ozone-free Xe lamp and an air mass AM 1.5 G filter. The lamp intensity was calibrated using an NREL-calibrated Si photodiode with a KG5 filter to mimic the spectral response of the organic solar cells to ensure that the integrated absorbed photon flux was the same for PCDTBT or P3HT as it would be under the 100 mW/cm^2 integrated AM 1.5 G spectrum. The spectral mismatch factor error with this method of calibration for our solar simulator is about 1% for P3HT and PCDTBT devices.

Aging apparatus: Detailed information concerning the testing apparatus is included in the Supporting Information. In brief, a water heated copper plate was used to hold the solar cells. The temperature of the stage was held at 37 ± 2 °C for the duration of the experiment and was monitored every 5 seconds. The temperature was monitored just below the solar cells and found to correlate very well with the water temperature. The variation between solar cells was also found to be <0.5 °C for the duration of the experiment. Illumination was provided by an LG sulfur plasma lamp (6,000K). The lamp has good spectral match to AM 1.5 solar spectrum in the visible with little power in the UV. The intensity was measured using an NREL-calibrated KG5 filtered silicon photodiode. Custom electronics were developed for Stanford University by Science Wares Inc. to allow individual control and monitoring of the solar cells. Each channel of the tester operates as an independent computer controlled four wire voltage source with separate force and sense lines. The tester operates through a LabVIEW interface that facilitates control of individual channel parameters and graphical monitoring of results while testing is in progress. Each cell was held on its maximum power point, which was dynamically adjusted every five seconds using a standard perturb and observe method. *J-V* curves were taken every hour.

Laser beam induced current (LBIC): Photocurrent maps were measured by using a custom-built LBIC system. In this system, samples are mounted to a 2-axis motorized translation stage (Standa 8MT173–20). Light from a continuous wave laser source (Spectra-Physics Stabilite 2017 argon ion laser) is focused down to a beam diameter of approximately 10 µm through a long working distance infinity corrected objective lens (Mitutoyo M Plan APO 20×/0.42). The laser beam is optically chopped (Stanford Research Systems SR540 Optical Chopper) while the sample stage moves in a two-dimensional pattern. The anode and cathode of the solar cell are connected to a transimpedance amplifer (Oriel), where the signal is converted to a voltage and subsequently sent to a lock-in amplifier (Stanford Research Systems SR830 DSP Lock-In Amplifier) for detection. The entire system is controlled via a LabVIEW interface.

Supporting Information

Supporting Information is available from the Wiley Online Library or from the author.

Acknowledgements

This publication was supported by the Center for Advanced Molecular Photovoltaics (Award No KUS-C1–015-21), made by King Abdullah University of Science and Technology (KAUST). We are grateful to Plextronics for their assistance in device fabrication and guidance with performing lifetime studies. We thank St-Jean Photochemicals for providing the polymer (PCDTBT) and LG for their support in providing the sulfur plasma lamps.

Received: March 15, 2011
Revised: March 31, 2011
Published online: April 20, 2011

[1] Y. Yang, G. Li, V. Shrotriya, J. Huang, Y. Yao, T. Moriarty, K. Emery, *Nat. Mater.* **2005**, *4*, 864.
[2] W. Ma, Yang, C., Gong, X., Lee, K., Heeger, A. J., *Adv. Func. Mater.* **2005**, *15*, 1617.
[3] Y. Liang, Z. Xu, J. Xia, S. T. Tsai, Y. Wu, G. Li, C. Ray, L. Yu, *Adv. Mater.* **2010**, *22*, E135.
[4] M. A. Green, K. Emery, Y. Hishikawa, W. Warta, *Prog. Photovolt: Res. Appl.* **2010**, *19*, 84.
[5] G. Dennler, M. C. Scharber, C. J. Brabec, *Adv. Mater.* **2009**, *21*, 1323.
[6] M. Jørgensen, K. Norrman, F. C. Krebs, *Sol. Energy Mater. Sol. Cells* **2008**, *92*, 686–714.
[7] C. J. Brabec, S. Gowrisanker, J. J. M. Halls, D. Laird, S. Jia, S. P. Williams, *Adv. Mater.* **2010**, *22*, 3839–3856.
[8] H. Neugebauer, C. Brabec, J. C. Hummelen, N. S. Sariciftci, *Sol. Energy Mater. Sol. Cells* **2000**, *61*, 35.
[9] F. Padinger, T. Fromherz, P. Denk, C. J. Brabec, J. Zettner, T. Hierl, N. S. Sariciftci, *Synth. Met.* **2001**, *121*, 1605.
[10] T. Jeranko, H. Tributsch, N. S. Sariciftci, J. C. Hummelen, *Sol. Energy Mater. Sol. Cells* **2004**, *83*, 247.
[11] S. Bertho, I. Haeldermans, A. Swinnen, W. Moons, T. Martens, L. Lutsen, D. Vanderzande, J. Manca, A. Senes, A. Bonfiglio, *Sol. Energy Mater. Sol. Cells* **2007**, *91*, 385.
[12] R. D. Bettignies, J. Leroy, M. Firon, C. Sentein, *Synth. Met.* **2006**, *156*, 510.
[13] J. A. Hauch, P. Schilinsky, S. A. Choulis, R. Childers, M. Biele, C. J. Brabec, *Sol. Energy Mater. Sol. Cells* **2008**, *92*, 727.
[14] M. O. Reese, A. J. Morfa, M. S. White, N. Kopidakis, S. E. Shaheen, G. Rumbles, D. S. Ginley, *Sol. Energy Mater. Sol. Cells* **2008**, *92*, 746.
[15] C. Lungenschmied, G. Dennler, H. N. S. N. Sariciftci, M. Glatthaar, T. Meyer, A. Meyer, *Sol. Energy Mater. Sol. Cells* **2007**, *91*, 379.
[16] R. Tipnis, J. Bernkopf, S. Jia, J. Krieg, S. Li, M. Storch, D. Laird, *Sol. Energy Mater. Sol. Cells* **2009**, *93*, 442.
[17] B. Zimmermann, U. Wurfel, M. Niggemann, *Sol. Energy Mater. Sol. Cells* **2009**, *93*, 491.
[18] S. K. Hau, H.-L. Yip, N. S. Baek, J. Zou, K. O'Malley, A. K.-Y. Jen, *Appl. Phys. Lett.* **2008**, *92*, 253301.
[19] M. T. Lloyd, D. C. Olson, P. Lu, E. Fang, D. L. Moore, M. S. White, M. O. Reese, D. S. Ginley, J. W. P. Hsua, *J. Mater. Chem.* **2009**, *19*, 7638–7642.
[20] S. H. Park, A. Roy, S. Beaupre, S. Cho, N. Coates, J. S. Moon, D. Moses, M. Leclerc, K. Lee, A. J. Heeger, *Nat. Photonics* **2009**, *3*, 297.
[21] N. Grassie, G. Scott, *Polymer Degradation and Stabilisation*, Vol. *1*, Cambridge University Press, New York **1985**.
[22] T. A. Bull, L. S. C. Pingree, S. A. Jenekhe, D. S. Ginger, C. K. Luscombe, *ACSNano* **2009**, *3*, 627.
[23] F. C. Krebs, R. Søndergaard, M. Jørgensen, *Sol. Energy Mater. Sol. Cells* **2010**.
[24] S. Cataldo, S. Fabiano, F. Ferrante, F. Previti, S. Patane, B. Pignataro, *Macromol. Rapid Commun.* **2010**, *31*, 1281.
[25] P. M. Sirimanne, T. Jeranko, P. Bogdanoff, S. Fiechter, H. Tributsch, *Semicond. Sci. Technol.* **2003**, *18*, 708.
[26] J. M. Kroon, M. M. Wienk, W. J. H. Verhees, J. C. Hummelen, *Thin Solid Films* **2002**, *403*, 223.